JOURNAL OF MATERIALS SCIENCE 23 (1988) 4477–4480

Investigation of the structural changes of the neutron irradiated amorphous alloy $Fe_{83}B_{17}$ by the method of partial radial distribution analysis

J. WEIS
Institute of Measurement and Measuring Engineering, Centre of Electro-physical Research, Slovak Academy of Sciences, Bratislava, Czechoslovakia

D. BARANČOK, I. ČERVEŇ
Department of Physics, Electrotechnical Faculty, Slovak Technical University, Bratislava, Czechoslovakia

The crystallization behaviour of amorphous $Fe_{83}B_{17}$ alloy after irradiation by thermal neutrons has been studied. The radiation effects on the atomic arrangement have been investigated by X-ray diffraction as well as by electrical resistance measurement. It was found that the crystallization of the alpha-iron was the eminent irradiation effect in the damaged region of the sample.

1. Introduction

The structural origin of amorphous materials has resulted in a promising forecast that these materials could be more resistant to the influence of radiation than crystalline ones. This forecast has been checked for various physical features.

The influence of neutron, electron and ionic radiation has been investigated on a large scale for rates and fluencies. The interest has focused mainly on investigation of the influence of neutron radiation with higher fluencies (e.g. 10^{17} to 10^{19} neutrons cm^{-2}), which caused the most significant structural changes. The materials frequently chosen are Fe–B and Fe–Ni–B alloys.

For instance, Nait Salem and Audouard [1] and Audouard *et al.* [2] studied the effects of 2.5 MeV electron irradiation and the influence of ^{10}B fission fragments on the electrical resistivity of amorphous and crystalline Fe–B alloys. Their results were interpreted in terms of the creation of well-defined defects of a vacancy type. Wagner *et al.* [3] and Gerling and co-workers [4–6] studied the neutron irradiation influence on the amorphous alloy $Fe_{40}Ni_{40}B_{20}$ in fluence rates from 10^{17} to 10^{20} neutrons/cm^{-2} at temperatures from 70 to 120° C. The neutron radiation consisted of fast and thermal neutrons with the intensity ratio 1 : 1. The impinging thermal neutrons, ^{10}B, caused nuclear fusion, ^{10}B (n, α) ^{7}Li + 2.3 MeV, and high energetic ions, ^{7}Li (0.9 MeV), and α particles (1.4 MeV) are produced. The authors state that the effect of ^{7}Li and α particles in creating structural changes is 10^4 times higher (in displacement per atom, dpa) than the effect of fast neutrons. Hayashi and Sakamoto [7] reported the irradiation effect of 40 keV helium-ion bombardment on the amorphous alloy $Fe_{80}B_{20}$. They showed that the α-iron phase appeared in the damaged region of the sample, whereas α-iron and iron borides were precipitated following annealing. The structural changes of the amorphous alloys $Fe_{98}Mo_2B_{20}$ and $Fe_{80}B_{20}$ after fast neutron irradiation have been studied by Grundy *et al.* [8]. The changes observed in glass and Curie temperatures were determined in the presence of structural and chemical defects.

The published results for various types of irradiation and various amorphous alloys do not fit a uniform scheme. It could be stated that the tendency of amorphous alloys to change on irradiation depends on their specific structure and on the type of irradiation. The forecast of good resistance of this alloy to the radiation effects does not seem to be valid universally.

The aim of this work which is connected with our previous publications [9–11] was to investigate the structural changes of the amorphous $Fe_{83}B_{17}$ alloy after irradiation with neutrons using X-ray diffraction partial radial distribution analysis, and also electrical resistance measurements.

2. Theory

A detailed analysis of the X-ray scattering intensity of amorphous $Fe_{83}B_{17}$ alloy has been carried out by X-ray diffraction using the anomalous scattering technique. The method of analysing the measured intensity was discussed previously [12, 13]. Only a short compilation of the equations required for the evaluations of the partial structure factors will be given here.

The scattering behaviour of an isotropic binary amorphous alloy can be described by three partial structure factors I_{11}, I_{22}, $I_{12} \equiv I_{21}$. These factors correspond to the diffraction of the two like-atom pairs (1–1 and 2–2) and one unlike-atom pair (1–2). A separation of these individual structure factors is one of the important aspects of the structural study of amorphous alloys.

0022–2461/88 $03.00 + .12

From partial structure factors, the total structure factor can be obtained

$$I(K) = \sum_{i=1}^{2}\sum_{j=1}^{2} W_{ij}(K) I_{ij}(K) \quad (1)$$

$$W_{ij}(K) = \frac{c_i c_j f_i(K) f_j^*(K)}{\sum_{i=1}^{2}\sum_{j=1}^{2} c_i c_j f_i(K) f_j^*(K)} \quad (2)$$

$$K = 4\pi/(\lambda) \sin\theta$$

where c_i is the concentration of the ith component in atomic fractions, $f_i(K)$ is the scattering factors of the atoms of the ith component, K is the diffraction vector, λ the X-ray wavelength, and θ the diffraction angle. The total structure factor is obtained from the coherently scattering intensity per atom $I_a(K)$ which follows from the measured intensity by a correction and normalization procedure. In this work we used the definition of a total structure factor given by Faber and Ziman [14]

$$I(K) = (I_a(K) - \langle f^2\rangle + \langle f\rangle^2)/\langle f\rangle^2$$

where

$$\langle f^2\rangle = \sum_{i=1}^{2} c_i f_i(K) f_i^*(K)$$

$$\langle f\rangle^2 = \sum_{i=1}^{2}\sum_{j=1}^{2} c_i c_j f_i(K) f_j^*(K)$$

The partial structure factor is defined by the generalized equation

$$I_{ij}(K) = 1 + \int_0^\infty 4\pi r^2(\varrho_{ij}(r)/c_j - \varrho_0)\frac{\sin(Kr)}{Kr}\,dr$$

where ϱ_0 is a mean atomic number per volume, $\varrho_{ij}(r)$ is a number of j atoms per volume element within a coordination sphere with radius r around an i atom. It is well known, that when the anomalous scattering of X-rays occurs, the above total scattering factor, $f_i(K)$, becomes complex in the following form

$$f_i(K) = f_{0i}(K) + \Delta f_i' + i\Delta f_i''$$

where $f_{0i}(K)$ corresponds to the atomic scattering factor for radiation with a frequency number higher than any absorption edge, whereas $\Delta f_i'$ and $\Delta f_i''$ are the real and imaginary components of the anomalous dispersion term. The anomalous dispersion terms $\Delta f_i'$ and $\Delta f_i''$ are dependent on the wavelength of the incident radiation. Therefore, measurements of the X-ray scattering intensity at two wavelengths near the absorption region of an i atom give two additional items of information on the total structure factor of a binary alloy due to Equations 1 and 2. These data, when coupled with those obtained from normal measurements using wavelengths out of the absorption region of an i atom permit the separation of the three partial structure factors.

The partial radial distribution functions can be defined as follows

$$G_{ij}(r) = 4\pi r(\varrho_{ij}(r)/c_j - \varrho_0)$$

$$= \frac{2}{\pi}\int_0^\infty K(I_{ij}(K) - 1)\sin(Kr)\,dK \quad (4)$$

$$\mathrm{RDF}_{ij}(r) = 4\pi r^2 \varrho_{ij}(r) \quad (5)$$

From the partial radial distribution function, $\mathrm{RDF}_{ij}(r)$, the partial coordination number, N_{ij}, can be calculated

$$N_{ij} = \int_{r_1}^{r_2} 4\pi r^2 \varrho_{ij}(r)$$

3. Materials and methods

Ribbons of amorphous alloy $Fe_{83}B_{17}$ (about 6 mm wide and about 0.0025 cm thick) were irradiated in the nuclear reactor channel to a fluence of 10^{18} neutrons cm^{-2}. The neutron radiation consisted of fast (2 MeV) and thermal neutrons with an intensity ratio of 2 : 1. The temperature of the samples did not exceed 100° C during irradiation. X-ray analyses were performed on the as-received amorphous sample as well as on the irradiated sample. All data were subject to the same collection and reduction procedures. The intensities were collected in transmission geometry with the flat graphite monochromator in the diffracted beam. The data were obtained by Mo$K\alpha$ and Co$K\alpha$ radiation with a statistical error less than 0.5%. The intensities were then corrected for background, polarization, absorption and Compton scattering. The residual fluorescent radiation of the samples could be eliminated from the measured intensity by the appropriate choice of a lower threshold voltage of the measuring channel. The intensities were then normalized to electron units [15].

The partial structure factors $I_{\mathrm{Fe-Fe}}(K)$, $I_{\mathrm{Fe-B}}(K)$ were then calculated from the two forms of Equation 1 for Mo$K\alpha$ and Co$K\alpha$ radiation. The structure factor of the boron atoms was neglected, because its contribution to the total structure factor was less than 0.2%. The partial factors of as-received amorphous and irradiated samples are presented in Figs 1 and 2, respectively. The partial distribution functions, $\mathrm{RDF}_{ij}(r)$, were then calculated from Equations 4 and 5. The computational errors were minimized by employing the procedures given by Kaplow *et al.* [16] with the modifications of Licheri *et al.* [17]. The resulting partial radial distribution functions, $\mathrm{RDF}_{ij}(r)$, for the as-received amorphous (dotted line) and irradiated

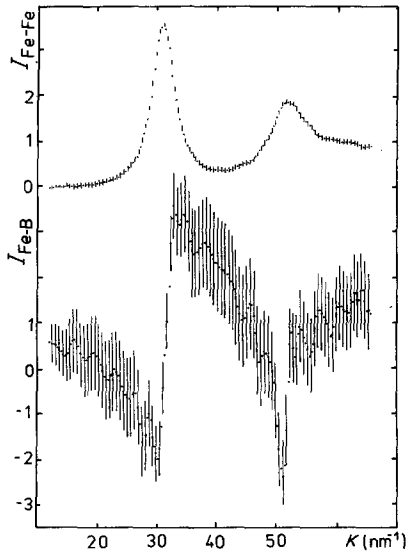

Figure 1 Partial structure factors of an as-received amorphous $Fe_{83}B_{17}$ sample.

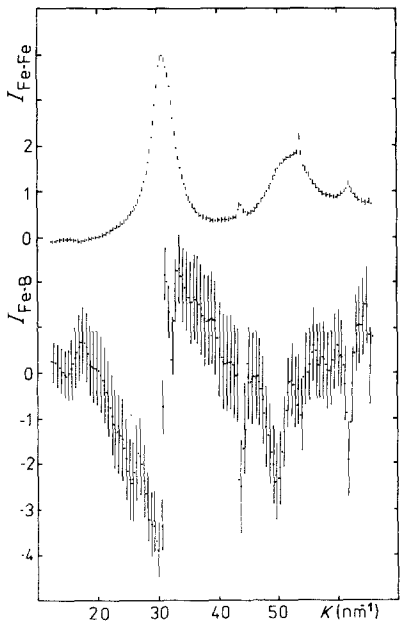

Figure 2 Partial structure factors of a sample irradiated by neutrons to a fluence of 10^{18} neutrons cm^{-2}.

(solid line) samples are presented in Figs 3a and b. Curve c, Fig. 3, represents the number of atoms of α-iron on the coordination spheres.

Electrical resistance measurements were made on the $Fe_{86}B_{14}$ and $Fe_{83}B_{17}$ samples. The size of the samples was 2 × 0.3 × 0.0025 cm^3. The voltage produced by constant current was measured using voltage contacts made from point-welded nickel wires. The sample holder allowed two samples to be measured simultaneously in the equal temperature regime. The heating rate used was 0.21 K min^{-1}. Fig. 4a shows the temperature dependence of the electrical resistance obtained simultaneously on as-received samples of $Fe_{83}B_{17}$ and $Fe_{86}B_{14}$, and simultaneous results for the as-received sample of $Fe_{86}B_{14}$ and the irradiated sample of $Fe_{83}B_{17}$ are shown in Fig. 4b.

4. Discussion

From X-ray and Mössbauer experiments, it was deduced [11] that α-iron phase appears in the damaged region of the sample after neutron irradiation.

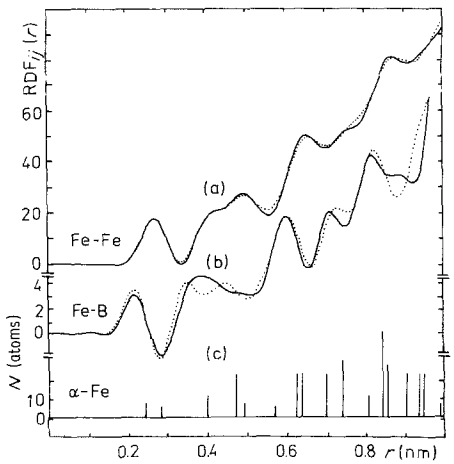

Figure 3 Partial radial distribution functions: (a) $RDF_{Fe-Fe}(r)$; (b) $RDF_{Fe-B}(r)$; (c) number of atoms of α-iron on the coordination spheres. (····) As-received amorphous sample, (——) sample irradiated by neutrons to a fluence 10^{18} neutrons cm^{-2}.

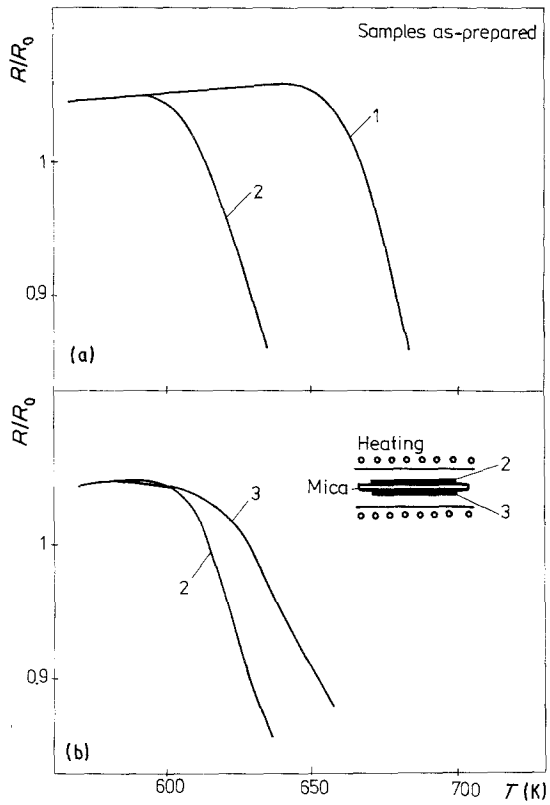

Figure 4 Electrical resistivity of Fe–B samples obtained by linearly increasing the temperature (0.21 K min^{-1}): (a) measurements on non-irradiated (1) $Fe_{83}B_{17}$ and (2) $Fe_{86}B_{14}$ taken simultaneously, (b) measurements on (3) irradiated $Fe_{83}B_{17}$ and (2) non-irradiated $Fe_{86}B_{14}$ taken simultaneously.

Detailed analysis of the Mössbauer spectra showed that the relative amount of α-iron was about 5%; the rest was amorphous. The resulting structure after irradiation has a different character compared to the structure of the annealed samples [9–11]. The crystallization of the α-iron phase is the eminent irradiation effect in the damaged region of the sample, whereas α-iron and iron borides are precipitated by subsequent annealing.

The radial distribution functions, RDF(r) (Fig. 3), show that the maxima and minima of the irradiated sample are more pronounced in comparison with the amorphous sample (dashed curve) particularly in the regions of α-Fe. This indicated the crystallization of the α-Fe. At the same time, the coordination number, Z_{Fe-Fe}, increased from the original value of 12.7 to 13.1 after irradiation.

This fact could be explained on the assumption that after neutron irradiation, areas of higher concentration and higher ordering of iron atoms are created in the amorphous material. In spite of this fact, that changes in the main maxima and coordination numbers are not too significant; this information is considered reliable, because Fe–Fe interaction has more than 93% contribution in the total structure factor. The more significant changes could be expected in $RDF_{Fe-B}(r)$, particularly in the first and second coordination spheres. The creation of areas of higher concentration and ordering of iron atoms is supported by changes in the main maxima of Fe–B interactions. Owing to the neutron irradiation, the main maximum become smaller after irradiation and simultaneously

the coordination number, Z_{B-Fe} decreases from 10.8 to 10.5, and Z_{Fe-B} decreases from 2.1 to 1.8. However, the most significant changes occurred in the shape of the second maximum, where two submaxima disappeared and one significantly simpler and more symmetrical maximum was created. From this fact it could be concluded that neutron irradiation caused enhanced dispersion of interatomic distances, r_{Fe-B}, outside the areas of higher concentration of iron atoms.

The simultaneous measurement of the electrical resistivity with linear increase in temperature shows that the crystallization begins and proceeds earlier in the sample with the smaller boron concentration (Fig. 4a). This kind of behaviour could be deduced immediately from the results obtained by the resistometric method on several compositions of Fe–B in work by Tóth [18] and Krempaský [19]. The simultaneous measurement on an irradiated sample of originally higher boron concentration, $Fe_{83}B_{17}$, and a non-irradiated sample with a concentration of $Fe_{86}B_{14}$, shows that the points of onset of crystallizations are practically identical (Fig. 4b).

Taking these facts into account, we proposed the following explanation of α-Fe crystallization. According to the analysis by Gerling and co-workers [3–5], the most significant influence on the structural change in the amorphous alloys, $Fe_{83}B_{17}$ is the reduction of thermal neutrons through the reaction

$$^{10}_{5}\mathrm{B} + {}^{1}_{0}\mathrm{n} \rightarrow {}^{7}_{3}\mathrm{Li} + {}^{4}_{2}\alpha$$
$$(0.9\,\mathrm{MeV}) + (1.4\,\mathrm{MeV})$$

The decomposition products ^{7}Li and α particles occupy the area originally occupied by ^{10}B, thus leaving behind an area deficient in boron. An area of enhanced concentration of iron atoms is created. The highly energetic ^{7}Li ions and particles produce secondary defects.

The crystallization of α-iron in the amorphous alloy $Fe_{80}B_{20}$ was also observed due to 40 keV He^{+} bombardment [7] and therefore the role of the secondary defects ^{7}Li and α particles seems to be significant and clearly plays a most important part by additional movement of boron atoms. The more homogeneous distribution of the second smallest interatomic distance, r_{Fe-B}, obtained by partial radial distribution analysis, is probably caused by boron atom diffusion, because the boron atom is significantly smaller than the iron atom and thus can more easily move through the interstitial space of the iron-atom matrix. The areas of higher iron-atom concentration create nucleation centres of crystallization of α-iron because the activation energy of the metallic glass, $Fe_{100-x}B_x$, rapidly decreases with falling boron concentration [20]. It could be assumed, that by slowing down the highly energetic ^{7}Li, α particles or boron atoms, the sample is heated for a short period, which can promote the growth of crystallization nucleii of α-iron. The fast decay of local temperature halts the process of crystallization before larger crystallites can form.

5. Conclusion

Two practical comments may be made. The amorphous alloys containing ^{10}B, involved in the possible reaction $^{10}\mathrm{B}(n, \alpha)^{7}\mathrm{Li} + 2.3\,\mathrm{MeV}$ due to the reduction of thermal neutrons, are less resistant to degradation of their characteristic properties caused by neutron irradiation than are other amorphous alloys. When producing amorphous alloys containing boron for environments with a higher neutron radiation, it is advisable to use another boron isotope (^{11}B) which is resistant to thermal neutrons. The partial radial distribution analysis method can contribute not only towards a better description of the amorphous structure, but also towards an explanation of the mechanism and kinetics of the transformation from the amorphous to the crystalline state.

References

1. M. NAIT SALEM and A. AUDOUARD, *Scripta Metall.* **16** (1982) 125.
2. A. AUDOUARD, J. BALOGH, J. DURAL and J. C. JOUSSET, *Rad. Effects* **62** (1982) 161.
3. R. WAGNER, R. GERLING and F. P. SCHIMANSKY, *J. Non-Cryst. Solids* **61**, **62** (1984) 1015.
4. R. GERLING, F. P. SCHIMANSKY and R. WAGNER, *ibid.* **61**, **62** (1984) 919.
5. R. GERLING and R. WAGNER, *J. Nucl. Mater.* **107** (1982) 311.
6. *Idem, Scripta Metall.* **16** (1982) 963.
7. N. HAYASHI and I. SAKAMOTO, *Phys. Lett.* **A88** (1982) 299.
8. P. J. GRUNDY, S. F. H. PARKER and G. A. JONES, *Nucl. Instrum. Methods* **209**, **210** (1983) 421.
9. J. WEIS and J. ČERVEŇ, *Phys. Status Solidi (a)* **76** (1983).
10. J. WEIS, D. BARANČOK and I. ČERVEŇ, *ibid.* **79** (1983) K117.
11. J. WEIS, F. GÁBRIŠ, I. ČERVEŇ and J. SITEK, *J. Mater. Sci. Lett.* **3** (1984) 278.
12. C. N. J. WAGNER, *J. Non-Cryst. Solids* **31** (1978) 1.
13. J. G. RAMESH and S. RAMASESHAN, *J. Phys. C Solid Stat. Phys.* **4** (1971) 3029.
14. T. E. FABER and J. M. ZIMAN, *Phil. Mag.* **11** (1965) 153.
15. J. KROGH-MOE, *Acta Crystallogr.* **A24** (1968) 321.
16. P. KAPLOW, S. L. STRONG and B. L. AVERBACH, *Phys. Rev.* **138** (1965) A1336.
17. G. LICHERI, G. PICCALUGA and G. PINNA, Redicanti del Seminario Della Facalta di Sciense della Universita di Cagliasi V-XLIII (1973) p. 67.
18. J. TÓTH, "Amorphous Metallic Materials", edited by P. Dumaj and P. Mrafko (Veda, Bratislava, 1980).
19. M. KREMPASKÝ, Thesis, Bratislava (1983).
20. F. E. LUBORSKY and H. H. LIEBERMANN, *Appl. Phys. Lett.* **33** (3) (1978) 253.

Received 18 November 1987
and accepted 29 April 1988